

PAPER • OPEN ACCESS

## Hydrogen resist lithography and electron beam lithography for fabricating silicon targets for studying donor orbital states

To cite this article: E. Crane *et al* 2018 *J. Phys.: Conf. Ser.* **1079** 012010

View the [article online](#) for updates and enhancements.



**IOP | ebooks<sup>TM</sup>**

Bringing you innovative digital publishing with leading voices  
to create your essential collection of books in STEM research.

Start exploring the collection - download the first chapter of  
every title for free.

# Hydrogen resist lithography and electron beam lithography for fabricating silicon targets for studying donor orbital states

**E. Crane, A. Kölker, T. Z. Stock, N. Stavrias, K. Saeedi, M. A. W. van Loon, B. N. Murdin, N. J. Curson**

London Center for Nanotechnology, University College London, Gower St, London, UK

E-mail: [e.crane@ucl.ac.uk](mailto:e.crane@ucl.ac.uk)

**Abstract.** Recently, phosphorous structures in silicon have been of interest theoretically and experimentally due to their relevance in the field of quantum computing. Coherent control of the orbital states of shallow donors in silicon has been demonstrated in bulk doped samples. Here we discuss the fabrication techniques required to 1) obtain patterned two dimensional dilute sheets of impurities in silicon of controlled doping densities 2) get them to act as targets for a terahertz laser. Scanning tunnelling microscope hydrogen lithography enables patterning of impurity features in silicon with a resolution from 1nm to tens of nm. Molecular beam epitaxy is used for a protective thin-film crystalline silicon growth over the impurity sheet. Electron beam lithography coupled with reactive ion etching allows features from tens to hundreds of microns to be etched into the silicon with 10 to 20nm resolution. The experimental readout is achieved via illumination of the silicon target by terahertz light and subsequent electrical detection. The electrical signal comes from coherent and non-linear excitations of the impurity electrons. This detection technique enables the precision condensed matter samples to remain intact after exposure to the free electron laser pulse.

## 1. Introduction

Investigating the properties of phosphorous impurities in silicon is crucial to forward the attempts which are being made to create entangling gates utilising the spins or atomic orbitals of the donor electrons[1][2][3]. While control of the phosphorous atomic orbital states by terahertz light has been demonstrated in 3D bulk doped Czochralski crystal grown silicon wafers [4][Chr], their control has not yet been demonstrated in two dimensions (2D). Deterministic placement of donors is only possible to a sufficiently a high degree of precision with scanning tunnelling microscope (STM) hydrogen lithography, which takes place in 2D (it can be layered to create deterministic 3D structures). For this reason, understanding 2D randomly doped impurity samples is a key stepping stone to deterministic positioning of entangling gates. Here we present the method developed to fabricate 2D dopant layer samples [5].

Coherent control of phosphorous Rydberg states in silicon has been demonstrated with optical and electrical detection [6][7].

The fabrication techniques used to grow the phosphorous 2D layer will first be presented. A range of lithographic techniques are used to transfer patterns to the surface of the samples: STM, hydrogen lithography and molecular beam epitaxy [11]. Secondly, the



Content from this work may be used under the terms of the [Creative Commons Attribution 3.0 licence](#). Any further distribution of this work must maintain attribution to the author(s) and the title of the work, journal citation and DOI.

techniques for accessing the buried 2D layer will be presented: electron beam lithography (EBL), reactive ion etching (RIE) and a hydrofluoric acid dip. Lastly, the method for electrical detection will be discussed.

The experiments are led collaboratively by the London Centre for Nanotechnology at University College London where the targets are produced and characterised, and by the University of Surrey and Radboud University in the Netherlands where the Free Electron Laser for Infrared eXperiments (FELIX) is used to perform the experiment [3].

## 2. Hydrogen lithography for the delta layer preparation

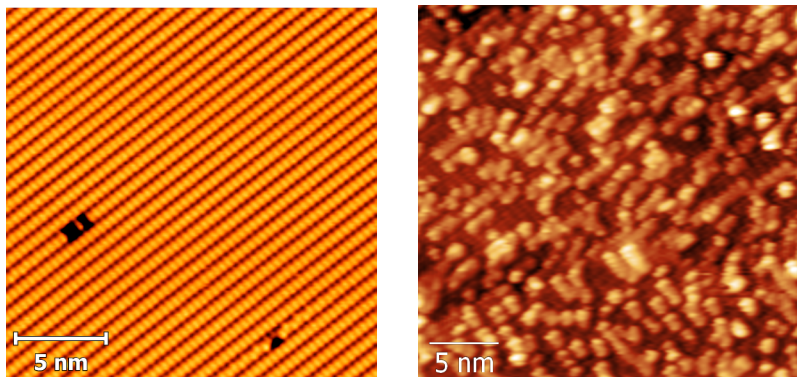


**Figure 1.** (left) Filled state STM image showing a clean Si(001)-2X1 surface. Silicon dimer rows run diagonally across the image and are interrupted by a low density of native defects. Pictured here are a 2+1 dimer vacancy defect, and a c-defect due to dissociation of water[12]. Image acquired with -2.0 V, 2 nA. Image courtesy of Taylor J.Z. Stock, London Centre for Nanotechnology, University College London. (right) Empty state STM image of an annealed Si(001)-PH<sub>3</sub> surface. The silicon is initially exposed to a monolayer saturation coverage of PH<sub>3</sub>, and then annealed at 350 C for 5 minutes. This anneal allows P atoms to incorporate into the surface lattice, and ejected silicon atoms are observed to form incomplete and isolated dimer rows on top, running perpendicular to the directions of the underlying surface dimer rows. Image acquired with +2.0 V, 2 nA.

In ultra-high vacuum (UHV), a dilute 2D layer of P or As donors is incorporated into the clean silicon crystal lattice. It's these 'isolated' dopants on which the terahertz experiments are performed. To establish a good metallic contact to the dilute 2D layer, highly conductive metallically doped phosphorous pads of 0.2 x 0.2 um are patterned on the same plane using STM hydrogen lithography. These 2D layers are overgrown with a protective layer of silicon. The metallic in plane pads are contacted using a process described in the next section, which utilises the technique of EBL.

The initial wafers are bulk n-type ( $10^{14}$  dopants per  $cm^3$  and above) Czochralski grown silicon. Deep etched orientation markers are transferred into the silicon (001) wafers via optical lithography to determine the location of the STM tip on the sample surface. All the wafers are in the [001] direction and nominally flat. They are only handled with ceramic tweezers in order to avoid contamination. They are then diced into 2 mm x 9 mm slices to fit into the Omicron variable temperature STM plates made of tantalum, molybdenum or ceramic.

After introduction into UHV in the preparation chamber, the sample holder is heated to 300°C, at which point the n-type silicon becomes conductive. Direct current is then passed through them until they reach temperatures of 600°C (confirmed by infra-red pyrometry), all the while keeping the pressure of the chamber below  $10^{-11}$  mBar. They are left to

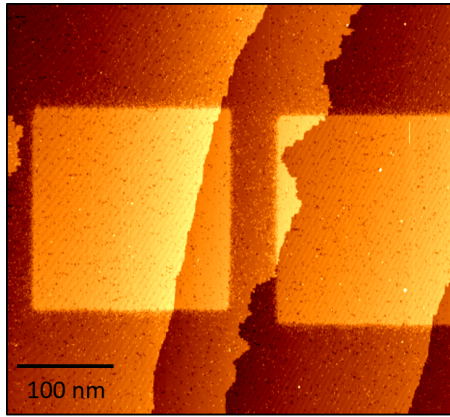


**Figure 2.** Hydrogen passivated silicon where two  $0.2\text{ }\mu\text{m} \times 0.2\text{ }\mu\text{m}$  squares have been desorbed with the STM tip. Desorption parameters: bias of 7.0 V, setpoint current of 1.0 nA, dose of 0.2 mC/cm and tip speed of 50.0 nm/s. Image acquired with -5V, 0.05nA. Image courtesy of A. Kölker, London Centre for Nanotechnology, University College London.

outgass overnight which removes the water absorbed onto both the sample and sample holder when they were in air [11].

The samples are flashed, ie. successively heated to temperatures of  $1150^\circ\text{C}$  four or five times, for up to 20 seconds at a time. This removes the native oxide on the surface of the silicon, as well as the impurities it accumulated before entering ultra-high vacuum [11]. The wafer is then ready to be processed in the STM chamber of base pressure  $10^{-11}$  mBar.

The metallic tip of the STM is brought within a few angstroms of the conductive sample surface. Applying a bias between the two induces a quantum mechanical tunnelling current to flow. While the tip is raster scanned across the surface of the sample, its height is altered in order to maintain the tunnelling current constant. Recording the positions of the tip at successive locations across the sample generates a map of the topography of the surface.

In order to ensure the sample is clean, randomly chosen small portions of the surface is scanned. Contamination may come from the tip or the sample holder (even in infinitesimal amounts, tungsten or nickel create dimer vacancy defects in the silicon surface) [12]. When the silicon is pristine, dimer rows are visible on the surface as in figure 1 (left).

Phosphine gas ( $\text{PH}_3$ ) is released onto the surface. The main sequence of dissociation is  $\text{PH}_2+\text{H}$ ,  $\text{PH}+2\text{H}$ , and  $\text{P}+3\text{H}$ , with the secondary sequence being  $\text{PH}+\text{H}$  to  $\text{P}+2\text{H}$  [13]. Phosphorous atoms are randomly distributed on the surface at a low coverage, the exact density of which can be determined by measuring the pressure of the gas in the chamber at the time of the gas exposure.

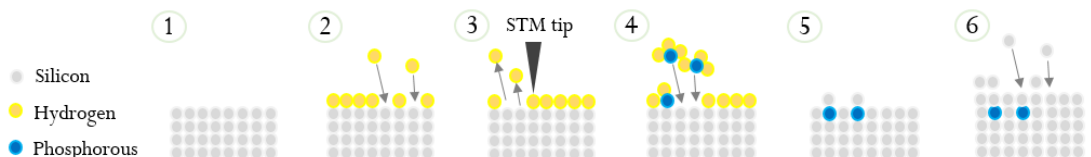


**Figure 3.** Process used in ultra-high vacuum scanning tunneling microscope chamber to carry out hyrdrogen lithography on clean silicon wafers, dose with phosphine gas and overgrow with silicon.

The sample is heated to  $\sim 350^\circ\text{C}$  for two minutes, incorporating all the phosphorous into the silicon. This process has taken place when bright protrusions (elevated atoms) are seen on the STM image which indicate that the phosphorous impurities have ejected the silicon atoms below them, which have then accumulated on the surface [11], see figure 1 (right).

The process of hydrogen lithography is used to define features on the silicon surface, as can be seen in figure 2. The sample is heated to 325°C with direct current passing through it. Exposure to hydrogen gas cracked by a hot tungsten rod results in a atomically thick layer of hydrogen covering the silicon. Applying a high voltage 8V and high setpoint currents of up to 3 nA between the STM tip and the sample creates enough energy to locally break the bond between the individual hydrogen atom and its supporting silicon [14]. The resulting half filled orbital protruding into the vacuum is called a dangling bond and is far more reactive than the surrounding robust hydrogen resist. Individual atoms of hydrogen can thus be removed to create atomically precise patterns [15]. Applying higher voltages and tip movement speeds enables larger areas to be desorbed, albeit with a lower precision. The technique is applicable for total areas of tens of nm to tens of microns and has also been demonstrated to enable placement of dopants to within 1nm precision [15].

Feedback controlled lithography has been developed and demonstrated to achieve high resolution nanopatterning [16]. The hydrogen resist can also be used as a hermetic layer to protect surfaces prepared in UHV from ambient conditions [17]. Placing two hydrogen passivated surfaces in contact with one another creates Van der Waals bonds between the hydrogen atoms and can protect the surfaces from being oxidised or contaminated for weeks [17]. It is also possible to identify previously positioned dopants underneath the hydrogen layer using the STM [18][19].

When exposed to phosphine gas only the exposed areas are reactive, not the ones protected by the hydrogen. The phosphine gas dissociates on the exposed areas, and remains local during the incorporation which is done by heating as previously discussed.

Molecular beam epitaxy enables a protective layer of silicon to be grown above the incorporated impurities. The sample is heated to 250°C by direct current while a silicon sublimation cell is heated to over 1000° and aimed at it. Single silicon atoms land on the surface and construct a thin crystalline film, following the base crystal structure of the sample. This technique can be used to grow tens to hundreds of nm of crystal on surfaces. Typically, the samples are encapsulated with 15 nm to 30 nm of epitaxial silicon. The deposition rate is of  $\approx 0.125$  nm/min.

A schematic of the entire process taking place in ultra-high vacuum can be seen in figure 3.

### 3. Electron Beam lithography for accessing the delta layer

In order to make electrical contacts to the buried nanostructures, EBL (or e-beam) is used in conjunction with RIE, and metal evaporation. The aim is to create small holes (vias), 70 nm in diameter and 60 nm deep into the silicon, which traverse the 0.2 x 0.2 um square patches of metallically doped phosphorous 15 nm to 30 nm below the surface. The sample is then exposed to a hydrofluoric acid dip and the vias are filled with aluminium to create metallic vias which maximises the surface area in contact with the phosphorous layer.

A thin organic film of resist coating the sample is exposed to a tightly focused and precisely controlled electron beam. The mask is directly defined by scanning the electron beam. The energy delivered to the resist in these regions chemically alters it [20]. When the coated sample comes into contact with a solvent (developer), the altered or non-altered regions are removed depending on if the resist is positive or negative respectively. EBL can create features with 10 nm - 20 nm resolution using polymer resist due to the size of the polymer molecules and the electron scattering during exposure [21]. The advantage of EBL over photo-lithography stems from the shorter wavelength of accelerated electrons compared to the wavelength of ultraviolet light.

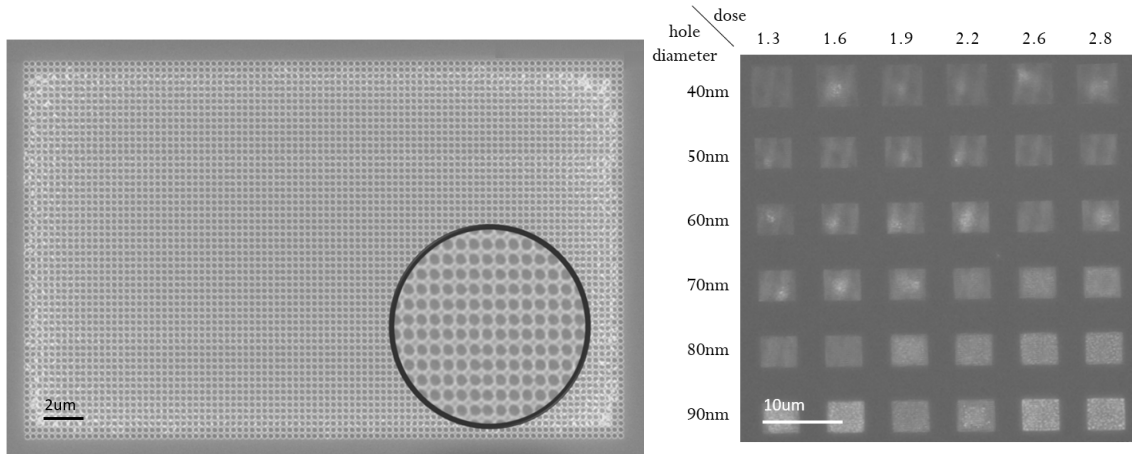


**Figure 4.** Scanning Electron Microscope (SEM) images of holes defined in resist using EBL. Beam Power used for SEM imaging and for EBL hole definition: 10 keV. Working distance: 10 mm. Doses are factors of the standard dose: 10  $\mu\text{A}/\text{cm}^2$ . (left) Etched holes of 70 nm diameter, 60 nm deep in the silicon sample. The black circle is a zoom on the holes. (right) A series of test holes etched into a test silicon sample.

The small, circular and stable electron beam is provided by an integrated Scanning Electron Microscope (SEM) [22]. To achieve high quality beam parameters UHV is used. A field emission source is used to create the electrons which scan the sample and expose the resist and is composed of one or two electrodes which extract and accelerate electrons pulled from a filament [20]. The beam brightness (equivalent to intensity in conventional optics) should be maximised to minimise exposure time, but in practice high resolution exposures are only achieved with lower intensities. Thinning the resist can improve the resolution of the features [21].

The pattern is written using software which is specific to the EBL equipment. As can be seen on figure 4, EBL has been used to create a mask containing circles in the resist. The resist is exposed to a beam of electrons of around 200 pA. The final dose corresponds to the amount of charge per unit area that the resist receives [20], it is obtained by multiplying the dose factor with the standard dose of 110  $\mu\text{A}/\text{cm}^2$ . The optimal dose found here was for holes with a diameter of 70 nm with a dose factor of 2.2, from which is the image displayed on figure 4 (left) was taken. The insides of the circles in pattern on the resist are then removed during the development stage. The resist-covered regions remain protected during further processing (until its removal). After cleaning, the sample is introduced into the RIE, which uses an etchant gas to remove the silicon in the exposed regions of the pattern.

The sample is covered in resist again, and contact pads are written onto the resist, aligned on the array of holes. After the resist has been developed, 150 nm of aluminium is deposited onto the surface. A lift-off removes the resist and covering aluminium around the pads. The silicon is left with aluminium contact pads with deep vias.

Test patterns with different exposure parameters and length scales must be carried out on a test sample beforehand such that the current beam parameters of the machine is accounted for, as is shown in figure 4 (right). The dose depends on the number of incoming electrons required to fully expose the resist and varies relative to the thickness, shape or area of the resist to be exposed.

EBL is also compatible with mono-atomically thick hydrogen, similar to STM hydrogen lithography (which can then have aluminium features grown onto the remaining hydrogen [21]); however, EBL hydrogen lithography is limited to 5 nm - 50 nm resolution.

#### 4. Electrical detection for non-destructive experimental result readout

The signal which arises due to the illumination of the low doped phosphorous 2D layer by the free electron laser beam can be readout optically or electrically [9]. Electrical detection is a more sensitive method and is therefore better adapted to samples where the phosphorous is confined to two dimensions, compared to the samples where the impurity species is introduced into the silicon during the melt, before the crystal is grown and therefore present in higher quantities per sample volume. Electrical readout, has been developed in silicon for the purposes of terahertz control of donors in silicon [6] and is possible with both 2D and 3D doping.

The 2p0 and 2p+- P states are split by the electron's anisotropic effective mass in silicon. Terahertz light tuned to the exact transition energy (39.19 meV)/ wavelength (31.64  $\mu\text{m}$ )/ frequency (9.48 Thz) selectively excites electrons from the insulating low doped phosphorous (located between the conductive 2x3um metallic pads in the 2D layer) from the 1s to 2p+- state. Once excited to this state, it can get excited into the conduction band by collisions with thermal phonons. It is electrically detected when a bias is applied across the sample. The beam size is between 0.02cm to 0.1cm, with cylindrical symmetry and a Gaussian intensity profile. For a 2D sample, this implies that around This technique, called photothermal ionisation spectroscopy (PTIS)[7], requires the sample to be electrically contacted. The mechanisms involved in PTIS are shown in figure 5 (left).

Typically, approximately 4 pA current per electron is detected. A graph of the current detected as a function of the free electron laser wavelength is shown in figure 5 (right), illustrating that it is possible to measure the number of donors excited to a specific state using electrical detection. The wavelengths at which the donor electrons to get from the 1s to the 2p0 and 2p+- states (corresponding to 36.4  $\mu\text{m}$  and 31.6  $\mu\text{m}$  respectively), are indicated on the graph.

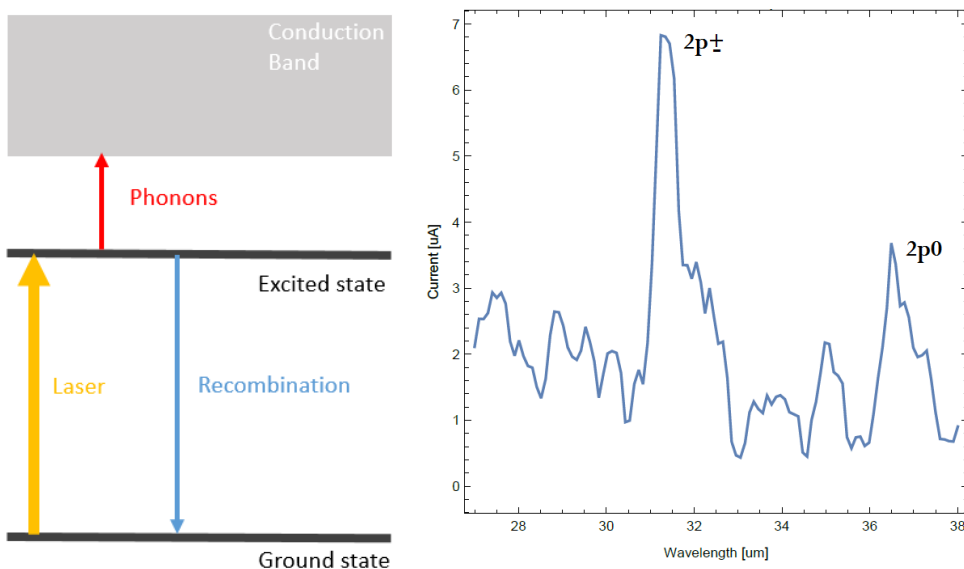


**Figure 5.** (left) Processes involved in Photo-Thermal Ionisation Spectroscopy. (right) Electrical signal as a function of terahertz laser wavelength in a contacted silicon sample containing a 2D phosphorous doped layer.

The samples can be current biased or voltage biased[6][7]. The picosecond dynamics can be accessed by voltage biasing the sample[6]. Electrical detection enables the samples to not be destroyed during the measurement. Using electrical detection, the homogeneous

phase decoherence rate has been demonstrated to be around around 160ps for the 2p+-state of phosphorous in silicon in a silicon sample of concentration  $2 \cdot 10^{-14}$  dopants per  $cm^3$  [9].

## Conclusion

Targets containing 2D phosphorous nanostructures can be made in silicon using a range of lithography, etching and overgrowth techniques. STM hydrogen lithography has up to 1 nm resolution and is a delicate process requiring ultra-high vacuum, whereas EBL using polymer resist has tens of nm resolution but can cover much larger areas. These techniques may be applicable in other areas of silicon laser target fabrication, such as those requiring shot power to be retained by the structure of the targets.

## Acknowledgements

We gratefully acknowledge the financial support from the UK Engineering and Physical Sciences Research Council [COMPASSS/ADDRFSS, Grant No. EP/M009564/1]. We thank the Stichting voor Fundamenteel Onderzoek der Materie (FOM) for the support of the FELIX Laboratory

## References

- [1] Stoneham A M, Fisher A J and Greenland P T 2003 *Journal of Physics: Condensed Matter* **15** L447–L451
- [2] Kane B E, 1998 *Nature* **393** 133–7
- [3] Stoneham A M 2003 *Physica B: Condensed Matter* **340–342** 48–57
- [4] Greenland P T, Lynch S A, van der Meer A F G, Murdin B N, Pidgeon C R, Redlich B, Vinh N Q and Aeppli G 2010 *Nature* **465** 1057–61
- [5] Matmon G, Ginossar E, Villis B J, Kolker A, Lim T, Solanki H, Schofield S R, Curson N J, Li J, Murdin B N, Fisher A J and Aeppli G 2018 *Phys. Rev. B* **97** 155306
- [6] Bowyer E T, Villis B J, Li J, Litvinenko K L, Murdin B N, Erfani M, Matmon G, Aeppli G, Ortega J M, Prazeres R, Dong L and Yu X 2014 *Appl. Phys. Lett.* **105** 021107
- [7] Greenland P T, Matmon G, Villis B J, Bowyer E T, Li J, Murdin B N, van der Meer A F G, Redlich B, Pidgeon C R and Aeppli G 2015 *Phys. Rev. B* **92** 165310
- [8] Vinh N Q, Greenland P T, Litvinenko K L, Redlich B, van der Meer A F G, Lynch S A, Warner M, Stoneham A M, Aeppli G, Paul D J, Pidgeon C R and Murdin B N 2008 *PNAS* **105** 10649
- [9] Tomaszewski P Jan Czochralski i jego metoda 2003 (Wrocław–Kcynia: Oficyna Wydawnicza ATUT)
- [10] Litvinenko K L, Bowyer E T, Greenland P T, Stavrias N, Li J, Gwilliam R, Villis B J, Matmon G, Pang M L Y, Redlich B, van der Meer A F G, Pidgeon C R, Aeppli G and Murdin B N 2015 *Nat. Comm.* **6** 6549
- [11] Tennant D M, Bleir A R and Wiederrecht G 2009 *Handbook of Nanofabrication* (Amsterdam: Elsevier)
- [12] Warschkow O, Schofield S R, Marks N A, Radny M W, Smith P V, and McKenzie D R 2008 *Phys. Rev. B* **77** 201305(R)
- [13] Ruess F J, Oberbeck L, Simmons M Y, Goh K E J, Hamilton A R, Hallam T, Schofield S R, Curson N J and Clark R G 2004 *Nano Letters* **4** 1969
- [14] Warschkow O, Curson N J, Schofield S R, Marks N A, Wilson H F, Radny M W, Smith P V, Reusch T C G, McKenzie D R and Simmons M Y 2016 *J. Chem. Phys.* **144** 014705
- [15] Walsh M A and Hersam M C 2009 *Annu. Rev. Phys. Chem.* **60** 193
- [16] Lyding J W, Shen T-C, Abeln G C, Wang C and Tucker J R 1996 *Nanotechnology* **7** 128
- [17] Schofield S R, Curson N J, Simmons M Y, Rueß F J, Hallam T, Oberbeck L and Clark R G 2003 *Phys. Rev. Lett.* **91** 136104
- [18] Grey F, Hermansson K 1997 *Appl. Phys. Lett.* **71** 3400
- [19] Brazdova V, Bowler D R, Sinthipharakoon K, Studer P, Rahnejat A, Curson N J, Schofield S R and Fisher A J 2017 *Phys. Rev. B* **95** 075408
- [20] Oberbeck L, Curson N J, Hallam T, Simmons M Y and Clark R G L 2004 *Thin Solid Films* **23** 464
- [21] Rius Sune G 2008 Electron Beam Lithography for Nanofabrication, Ph.D (Universitat Autònoma de Barcelona)
- [22] Masu K and Tsubouchi K 1994 *J. Vac. Sci. Technol. B* **12** 3270